Korean Journal of Chemical Engineering
https://doi.org/10.1007/s11814-025-00517-x

ORIGINAL ARTICLE

Lauroyl Lysine Continuous Injection Synthesis via Schotten–Baumann Reaction pH Optimization as Synthetic Amino Acid Derivative

Min Jeong Park[1] · Tae Yeon Kim[1] · Sang Jun Lee[1] · Seo Yeon Jung[1] · Shin Hum Cho[1]

Received: 11 April 2025 / Revised: 1 July 2025 / Accepted: 7 July 2025

Abstract

This research focuses on identifying optimal synthesis conditions for lauroyl lysine, an amino acid derivative widely used in the cosmetics industry. The effect of pH on reaction rate and selectivity was quantitatively assessed through systematic variations within the range between pH 10 and pH 13, and the reaction conditions were subject to a continuous slow precursor injection technique as alternative to batch-type reaction. This results in optimal pH conditions and the establishment of a synthesis via Schotten–Baumann reaction process on a laboratory scale, yielding from 97.77 to 55.20% range. This study will contribute to maximizing the industrial scale-up synthesis efficiency of lauroyl lysine and expanding its application potential in the cosmetics industry, reducing manufacturing costs and expect the possibility of commercial production.

Keywords Chemical engineering · Amino acid · Organic chemistry · Industrial chemistry · Amino derivative

Introduction

Lauroyl lysine is a high-performance amino acid derivative synthesized through the condensation reaction of lauric acid and lysine and is attracting attention as a sustainable cosmetic ingredient with potential as a high-value-added material with the growing demand for naturally derived ingredient biocompatibility in the cosmetics industry. However, in the synthesis process of lauroyl lysine, establishing the conditions for maximizing reaction efficiency and product quality is still a significant challenge to be solved. The biocosmetics market is rapidly expanding in commercial and industrial fields in synthetic amino acid derivatives. Particularly, organic compounds such as lauroyl lysine are used as important ingredients in various cosmetics, including lotion, cream, and hair care products. With the increasing use of these organic compounds, it is essential to ensure the biochemical compatibility of the products. Also, the synthesized amino acid derivative material must undergo evaluation process to demonstrate its efficiency in maximizing chemical yield while minimizing waste, ensuring cost-effective production. This optimization must be achieved before the final product reaches the market and is a crucial factor in enhancing economic viability and competitive advantage.

The functional groups present between organic carbon and amino compound are highly sensitive to pH reactivity conditions in Schotten–Baumann reaction, especially on amino acids. Amino acids are organic compounds characterized by the presence of an amino group ($–NH_2$) and a carboxyl group (–COOH), making them fundamental building blocks of proteins in biological systems. They exhibit unique chemical properties due to their amine and carboxyl functional groups. Amino acids, which act as pillars of amino derivative compound biomaterials, are widely used in synthetic reactions, such as protein detection in the field of organic chemistry and biology.

In this study, the reaction conditions were subdivided by setting the range of pH 10–13 in the synthesis of lauroyl lysine, and the Schotten–Baumann reaction efficiency and purity of the product were analyzed under each pH condition. In particular, the goal was to quantitatively evaluate

✉ Shin Hum Cho
shinhum@kmu.kr

Min Jeong Park
alswjd696969@naver.com

Tae Yeon Kim
dc10061@naver.com

Sang Jun Lee
isangjun913@gmail.com

Seo Yeon Jung
fdsa02q@naver.com

[1] Department of Chemical Engineering, Keimyung University, Daegu 42601, Republic of Korea

Published online: 17 July 2025

the effect of pH on reaction rate and selectivity in the process of condensation reaction to identify the optimal pH conditions. This pH analysis provides the basis for stable and reproducible synthesis of lauroyl lysine and provides an important design criterion for scale-up to large-scale production. In addition, this study established a highly efficient synthesis process on the lab scale using continuous slow precursor injection technique as alternative to typical batch-type reaction to control side reactions related to excessive pH changes during the reaction. We examine the possibility of cost reduction through the scale-up process and develop economical mass production technology to contribute to the development of high-value-added products based on lauroyl lysine. This paper aims to combine the basic research of the reaction of lauroyl lysine synthesis under pH conditions with the possibility of mass production, and to promote its application as a high-performance raw material in the cosmetics industry.

For product materials evaluation study, the resulting synthesis process and its properties of lauroyl lysine were characterized. The structural properties of the compounds were confirmed through Fourier transform infrared spectroscopy (FTIR), scanning electron microscopy (SEM), and nuclear magnetic resonance (NMR) analysis. Furthermore, vibrational spectroscopic data were further evaluated through ab-initio quantum mechanical simulations. In addition, the optimal synthesis conditions were explored by comparing the synthesis yields under various pH conditions, and the potential safety as a cosmetic ingredient was investigated through this. These studies are an important step in confirming that lauroyl lysine amino acid derivative product evaluation in chemical engineering commercial applicability.

Experimental Method

Materials

Sodium hydroxide (bead, 98.0%) and ninhydrin (2,2-dihydroxyindan-1,3-dione, 98%) were purchased from Samchun Chemical (Republic of Korea). L-lysine (> 99%) was purchased from CJ CheilJedang Corporation (Republic of Korea). Lauroyl chloride ($CH_3(CH2)_{10}COCl, > 99\%$) was purchased from Lee'N Chemical (Republic of Korea). Sulfuric acid (95.0–98.0%) was purchased from Sigma-Aldrich. Ethyl alcohol (99.5%) was obtained from Daejung Chemical (Republic of Korea).

Lauroyl Lysine Synthesis

In a three-neck round bottom flask, 20 mmol (2.29 g) of L-lysine amino acid was added, followed by dissolution in 50 ml of deionized water. The pH of the solution was adjusted to pH 10 using a 10% w/v NaOH solution to ensure complete dissolution of L-lysine. Into this solution, 20 mmol (4.66 ml) of lauroyl chloride was continuously injected slowly at a rate of 0.08 ml/min over the course of 1 h at room temperature (25 °C). During the continuous flow addition of lauroyl chloride, the pH was consistently maintained at pH 10 by gradual addition of 10% wt. NaOH solution, with continuous stirring to promote uniform reaction conditions. After the complete addition of lauroyl chloride, the basic reaction mixture was neutralized to pH 7 using a 30% wt. sulfuric acid solution. Subsequently, 50 ml of ethanol was added to the product, thoroughly vortexed, and centrifuged at 4000 rpm for 3 min into centrifuge tube to isolate the solid white precipitate. The separated precipitate was then transferred into 20 ml of deionized water, vortexed again, and centrifuged under the same centrifuge conditions. The separated product was dried at room-temperature ambient air overnight to obtain the final product. The obtained precipitate was further purified by resuspension in 20 ml of acetone, followed by vacuum filtration to remove any remaining impurities. The filtered product was then dried at room temperature to yield the final purified lauroyl lysine. The synthesis of lauroyl lysine was first performed on a 20 mmol scale, as described above. For the scale-up experiments, the reaction was carried out on a twofold (40 mmol), threefold (60 mmol), and fourfold (80 mmol) scale. In each case, all reagent amounts and solvent volumes were adjusted proportionally, and the total reaction time was maintained at 1 h. Accordingly, the addition rate of lauroyl chloride was proportionally increased to ensure complete addition within the same time frame (i.e., 0.16 ml/min at 40 mmol, 0.23 ml/min at 60 mmol, and 0.31 ml/min at 80 mmol), while other reaction conditions, such as pH, temperature, and stirring speed, were kept constant.

Ninhydrin Test Process

Ninhydrin test (JIS K 8870:2017) was performed to verify lauroyl lysine amino acid derivative product retains amino acid groups. Ninhydrin is a dye compound that reacts with amino acids to induce a color change that confirms the presence of an amine group, producing its characteristic purple and amber color. If color change appears during the reaction, it indicates that amino acid group has been successfully retained in the resulting compound. This allows us to verify the inclusion of amino acids in the experimental sample. The ninhydrin test experiment was performed on lauroyl lysine synthesized under four different pH conditions (pH 10 ~ 13). 0.2 g of ninhydrin was dissolved in 10 mL of ethanol to create a 2.0% wt. ninhydrin solution. 0.1 mL of ninhydrin solution was prepared by dispersing 0.1 g of synthesized lauroyl lysine

product in 25 mL of deionized water. Using a vacuum oven, the mixture was heated to 80 °C for 5 min, and then cooled for 5 min to observe color change [1].

Fourier-Transform Infrared Spectroscopy (FTIR)

Lysine sample was analyzed using the attenuated total reflectance (ATR) mode in FTIR. The analysis was performed using a Nicolet Summit FTIR Spectrometer (Everest ATR mode, Green Bay, WI, USA).

Scanning Electron Microscope (SEM)

A powder solid lauroyl lysine sample was placed onto carbon tape and evenly spread over the surface. The sample was then coated with platinum (Pt) using an ion coater for approximately 3 min. SEM images were obtained using a Hitachi SU8230 scanning electron microscope (Chiyoda City, Japan) at an accelerating voltage of 15.0 kV.

Infrared Vibrational Spectroscopy Ab Initio Simulations

The molecular structure of lauroyl lysine was optimized using the Avogadro 2 (1.100.0 release) program geometry optimization. Based on the geometry optimized structure, vibrational analysis was performed using the ORCA 6.0 quantum chemical simulation package with Perdew–Burke–Ernzerhof functionals and Ahlrichs def2 family basis sets (PBE OPT def2-SVP def2/J FREQ). [2] The theoretically calculated FTIR vibrational peaks were then compared with the experimentally obtained FTIR spectrum.

Discussion

Figure 1a compares the reaction solutions before and after lauroyl lysine synthesis. The reaction solution before synthesis (left) is transparent, indicating that the reactants lysine is uniformly dissolved and lauroyl chloride precursors are distributed in solution under liquid phase. On the other

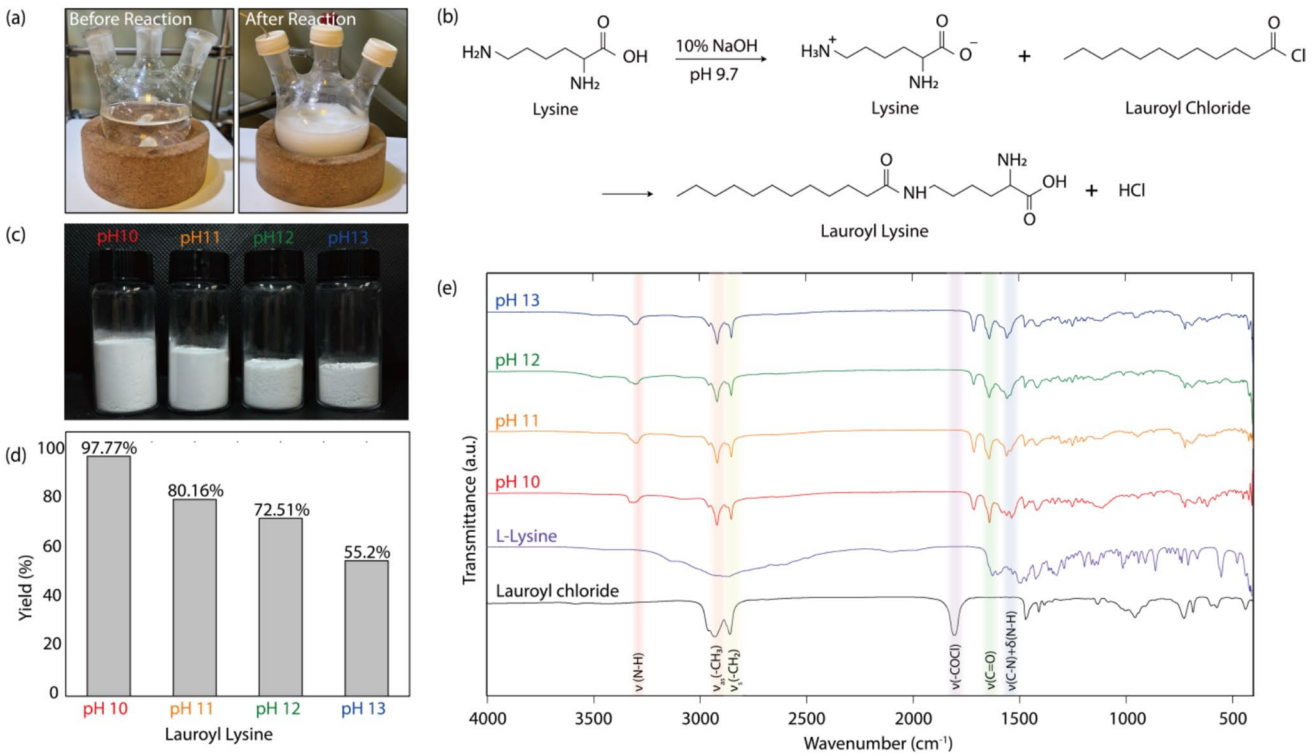

Fig. 1 **a** Visual comparison before and after the synthesis of lauroyl lysine. The solution changes from a transparent state (left) before synthesis to an opaque milky suspension (right) after synthesis, indicating the formation of lauroyl lysine. **b** Schotten–Baumann reaction mechanism of lauroyl lysine synthesis. The α-amino group in lysine undergoes a nucleophilic substitution reaction with lauroyl chloride, leading to the formation of lauroyl lysine. **c** Visual comparison of lauroyl lysine synthesized at varying pH values (10, 11, 12, and 13). As the pH increases, the amount of synthesized lauroyl lysine decreases. **d** Lauroyl lysine yield as a function of pH. The highest yield is optimized and observed and at pH 10, and the yield decreases as pH increases. **e** FTIR spectra of lauroyl chloride, L-lysine, and lauroyl lysine synthesized at pH 10 ~ 13. The characteristic peaks corresponding to amide bond (C = O) and lauroyl carbon chain groups (-CH_2, -CH_3) are observed, while acyl halide (-COCl) group is reduced after synthesis

hand, the solution after synthesis (right) changed to opaque and milky white suspension form, which can be visually confirmed that lauroyl lysine product was condensed and precipitated in the solution [3]. These changes suggest that due to the low water-solubility of lauroyl lysine, the product was separated from the solution after the reaction was completed [4].

Figure 1b shows the reaction synthesis mechanism of lauroyl lysine. The reaction is carried out by a Schotten–Baumann nucleophilic substitution reaction between the α-amino group of lysine and the lauroyl chloride [5, 6]. In the initial stage, the carboxyl group of lysine is deprotonated and converted into an anion form using a NaOH solution, and the reaction pH is adjusted to 10 to optimize it [7]. The pH 10 synthetic condition is higher than the pH 9.7 isoelectric point where lysine is present in the form of zwitterion, making it nucleophilic as the α-amino group remains aprotonized [8, 9]. When lauroyl chloride reactant is added, the acyl chloride group acts as a breakaway group, and the amino group (-NH_2) in lysine makes a nucleophilic attack on the carbon center of lauroyl chloride acyl group, and lauroyl lysine final product is formed. Along with the end-product, HCl is produced as a by-product, which can be neutralized within the reaction solution [5]. Acid base pH plays an important role in this reaction, and if pH is too low, the amino group in lysine will protonize and reduce its nucleophilicity. If pH is too high, it will likely cause lauroyl chloride acyl halide group to hydrolyze into impotent lauric acid reactant, resulting in an inefficient reaction for Schotten–Baumann reaction condensation.

Figure 1c shows a visual comparison of lauroyl lysine product synthesized under pH 10 ~ 13 conditions. Synthesis was carried out at pH 10, 11, 12, and 13, and the lauroyl lysine precipitate solid product gradually decreases as pH increases. As reaction pH becomes too high, the hydrolysis reaction in lauroyl chloride acyl chloride to carboxylic acid increases. This results in an increase for non-specific side reactions other than the intended target synthesis reaction, resulting in a lower yield in end-product [5, 10]. Lauroyl lysine synthesized at pH 10 showed the highest yield amount, while relatively lower solid precipitate was found at pH 13 [11]. This is believed to reflect the rapid hydrolysis of lauroyl chloride at high pH, resulting in a deterioration in reactivity into lauric acid side product.

Figure 1d is a quantitative graph of the yield of lauroyl lysine according to function of pH. The highest yield was 97.77% at pH 10, with a tendency to decrease as the pH increased. The yield was 80.16% at pH 11, 72.51% at pH 12, and 55.20% at pH 13. This indicates that pH 10 is the most suitable condition for lauroyl lysine synthesis, as it is above the isoelectric point of lysine (pH 9.7). If the pH is too high, however, increased hydrolysis of lauroyl chloride may occur, leading to reduced reaction efficiency [12]. On the other hand, at pH levels below 9.7, lysine was observed to have poor solubility in the reaction medium, which could limit its reactivity. Therefore, pH 10 or higher was selected as the optimal condition in this study. Particularly, at pH 13, yield was reduced by less than half, suggesting that reactivity can deteriorate rapidly at higher pH. Therefore, the pH range of 10 can be considered as the optimal condition for the synthesis of lauroyl lysine, while accommodating the isoelectric point limit for the lysine amino acid precursor [13]. The tendency for yields to decrease at higher pH can also be interpreted in terms of reaction kinetics. Previous studies of amide bond formation involving fatty acid derivatives have reported activation energies (E_a) in the range of 10–50 kJ/mol, which are generally considered low and favorable for efficient synthesis [14, 15]. For example, amidation reactions between lauric acid esters and ethanolamine or diethanolamine exhibited activation energies as low as 10.3 to 50.2 kJ/mol, depending on the catalyst and temperature. In the context of lauroyl lysine synthesis, this low energy barrier may contribute to the high reactivity observed at pH 10, but may be offset by side reactions and hydrolysis as pH increases. Therefore, it seems important to maintain conditions that preserve this low energy reaction pathway (e.g., around pH 10) to maximize yield and minimize by-product formation.

Figure 1e compares the FTIR spectra of synthesized lauroyl lysine (pH 10 ~ 13), L-lysine, and lauroyl chloride. In the FTIR spectrum of lauroyl chloride, a strong absorption band appears at around 1750 cm^{-1}, corresponding to the C = O-stretching vibration characteristic of acid chlorides [12]. In addition, symmetric stretching vibrations of $–CH_2–$ and $–CH_3$ in the region of 2800–3000 cm^{-1} are clearly observed, which reflects the characteristics of the lauroyl carbon chain group. In the FTIR spectrum of L-lysine, there is a strong N–H symmetric stretching vibration peak in the range of 3200–3500 cm^{-1}, which is related to the bonding of amino groups and hydrogen. In addition, C = O-stretching oscillations are observed around 1600 cm^{-1}, which show the main characteristics of α-amino acids [16]. In the FTIR spectrum of the synthesized lauroyl lysine (pH 10 ~ 13), amide-bound (C = O) stretching oscillations were clearly seen around 1630–1660 cm^{-1}, indicating that lauroyl chloride and L-lysine successfully reacted to form amide bonds [17]. There is a strong N–H-bond characteristic peak at 3300–3500 cm^{-1}, which is associated with the amino group of lauroyl lysine. Due to its low solubility in common solvents, such as water, methanol, and acetonitrile, lauroyl lysine could not be evaluated for purity by the conventional HPLC. Instead, the purity of the synthesized lauroyl lysine was evaluated using FTIR spectral matching. The relative purity of each sample was assessed based on the spectral matches derived from the FTIR fingerprint region. The matches compared to the lauroyl lysine standard were 99.8% at pH 10, 58.1% at pH 11, 54.5% at pH 12, and 44.2% at pH

13. These matches support the structural integrity and high purity of the final compounds.

To evaluate the microstructure of lauroyl lysine solid precipitate powder product, the samples synthesized under pH 10 ~ 13 condition are analyzed using SEM. Each sample was observed at the same 15 kV acceleration voltage, and the particle morphology and surface properties were observed at different magnifications. Figure 2a, b shows SEM images of lauroyl lysine synthesized at pH 10. The particles observed at the 500 × magnification at Fig. 2, appear to be relatively evenly dispersed, and a large number of powder particles with irregular polyhedral-like shapes can be seen. This shows that the crystallization of lauroyl lysine precipitate was stable under pH 10 reaction condition. Figure 2b, taken at a higher magnification of 10,000x, shows that the surface structure of individual particles is stacked in a multi-layered structure with plate-like crystals. This indicates that lauroyl lysine has a relatively high crystalline structure and tends to form a layered laminate formation. In addition, the surface is smooth and contains coarse crystals, suggesting that the synthesized lauroyl lysine maintains a relatively high purity [12].

Figure 2c, d shows SEM images of lauroyl lysine synthesized at pH 11. The particles observed at the 500 × scale (Fig. 2c) appear slightly more agglomerated than those at pH 10, and the boundaries between individual particles are relatively unclear. Figure 2d, taken at 5,000 × magnification, shows branched or fibrous structures. This means that at pH 11, lauroyl lysine showed a more uneven growth pattern during the crystallization process. These fibrous structures are interpreted to have a relatively high rate of crystallization formed by minute changes in pH. In some areas, it contains coarse and dense crystals, and it is judged to maintain relatively high crystallinity even at pH 11 [12].

Figure 2e, f shows SEM images of lauroyl lysine synthesized at pH 12. At the 500 × magnification (Fig. 2e), the particles showed greater cohesion compared to pH 10 and 11, and some particles were distributed in irregular shapes [18]. This means that the reactivity of lauroyl lysine is further disrupted during the production process at pH 12, and aggregates of particles are formed by changes in solubility [18]. Figure 2f, taken at 5000 × magnification, shows a more pronounced porous structure. This morphology is considered to result from incomplete dissolution of lysine under high pH conditions [19]. According to the ninhydrin test, some of the lysine powder remained as undissolved or by-product forms at pH 12 and 13 [20]. This suggests that lauroyl lysine was not fully dissolved in either water or the ninhydrin solution, leading to the presence of amorphous and porous structures. In addition, the surface is relatively rough and uneven, and it appears to contain some amorphous components. This suggests that under high pH conditions, lauroyl chloride may have partially hydrolyzed, resulting in the formation of impurity side products [21].

Figure 2g, h shows SEM images of lauroyl lysine synthesized at pH 13. In Fig. 2g, taken at 300 × magnification, particles appear more irregular in shape and distribution compared to other pH conditions [22]. This suggests that the hydrolysis of lauroyl chloride at pH 13 may have been further accelerated, resulting in incomplete crystallization

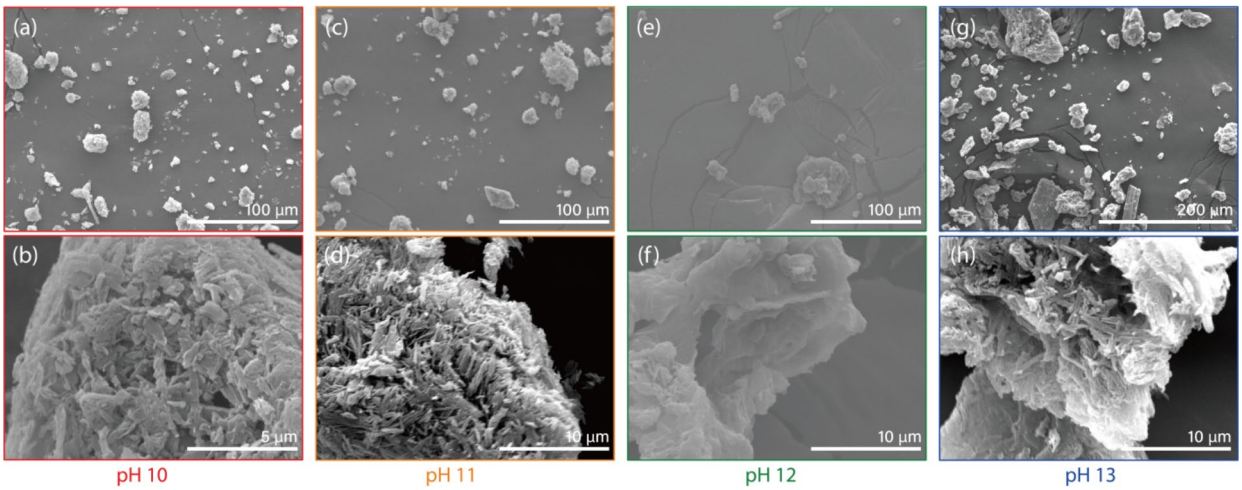

Fig. 2 SEM images of lauroyl lysine synthesized at varying pH conditions. **a**, **b** Morphology of lauroyl lysine synthesized at pH 10, captured at 500 × (**a**) and 10 k × (**b**) magnifications. The particles appear well-defined and uniformly distributed. **c**, **d** SEM images of lauroyl lysine synthesized at pH 11, captured at 500 × (**c**) and 5.0 k × (**d**) magnifications. The structures exhibit a more aggregated and fibrous morphology compared to pH 10. **e**, **f** SEM images of lauroyl lysine synthesized at pH 12, captured at 500 × (**e**) and 5.0 k × (**f**) magnifications. The particles display irregular, sheet-like structures, indicating a change in crystallinity. **g**, **h** SEM images of lauroyl lysine synthesized at pH 13, captured at 300 × (**g**) and 5.0 k × (**h**) magnifications. The morphology becomes more disordered, with larger aggregated structures, suggesting decreased crystalline particle synthesis at higher pH

of lauroyl lysine [18]. Figure 2h at 5,000 × magnification shows a fibrillar or layered structure, but with a relatively rough and uneven surface. This means that at high pH, lauroyl lysine undergoes incomplete crystallization, and the growth of the crystals proceeds uncontrolled [23]. These structural properties may be the effect of the rapid decline in the yield of lauroyl lysine at pH 13 [21].

Through SEM analysis, the microstructure changes of lauroyl lysine were qualitatively evaluated according to pH changes. At pH 10, it has a spherical or plate-like structure, exhibiting uniform crystallinity. At pH 11, the fibrous structure developed, and some aggregation increased. At pH 12, porosity increased markedly, and amorphous surfaces were identified. Finally, at pH 13, the inhomogeneity of crystal growth increased, and aggregation and amorphous phases intensified. These results suggest that pH 10 is a condition that can optimize the crystallization of lauroyl lysine. The powder particle surface crystallinity of lauroyl lysine decreases as the pH increases, and the structural inhomogeneity tends to increase.

Figure 3a shows the results of a ninhydrin test conducted on lauroyl lysine synthesized under four different pH conditions (pH 10, 11, 12, and 13). The samples were arranged in order from left to right, demonstrating the reaction at each pH conditions. To perform the ninhydrin test, a ninhydrin solution was prepared by dissolving 0.2 g of ninhydrin (2,2-dihydroxyindan-1,3-dione) powder in 10 mL of ethanol to create a 2.0% wt. solution [24–26]. For the experiment, 0.1 g of synthesized lauroyl lysine was dissolved evenly in 25 mL of deionized water. Subsequently, 0.1 mL of the prepared ninhydrin solution was added using a micropipette. The mixture was then heated to 80 °C, maintained at this temperature for 5 min, and subsequently cooled for another 5 min [27]. This procedure was repeated for each lauroyl lysine sample synthesized under varying pH conditions.

The ninhydrin test is a standard method used to identify the presence of amino acids and proteins by exploiting the

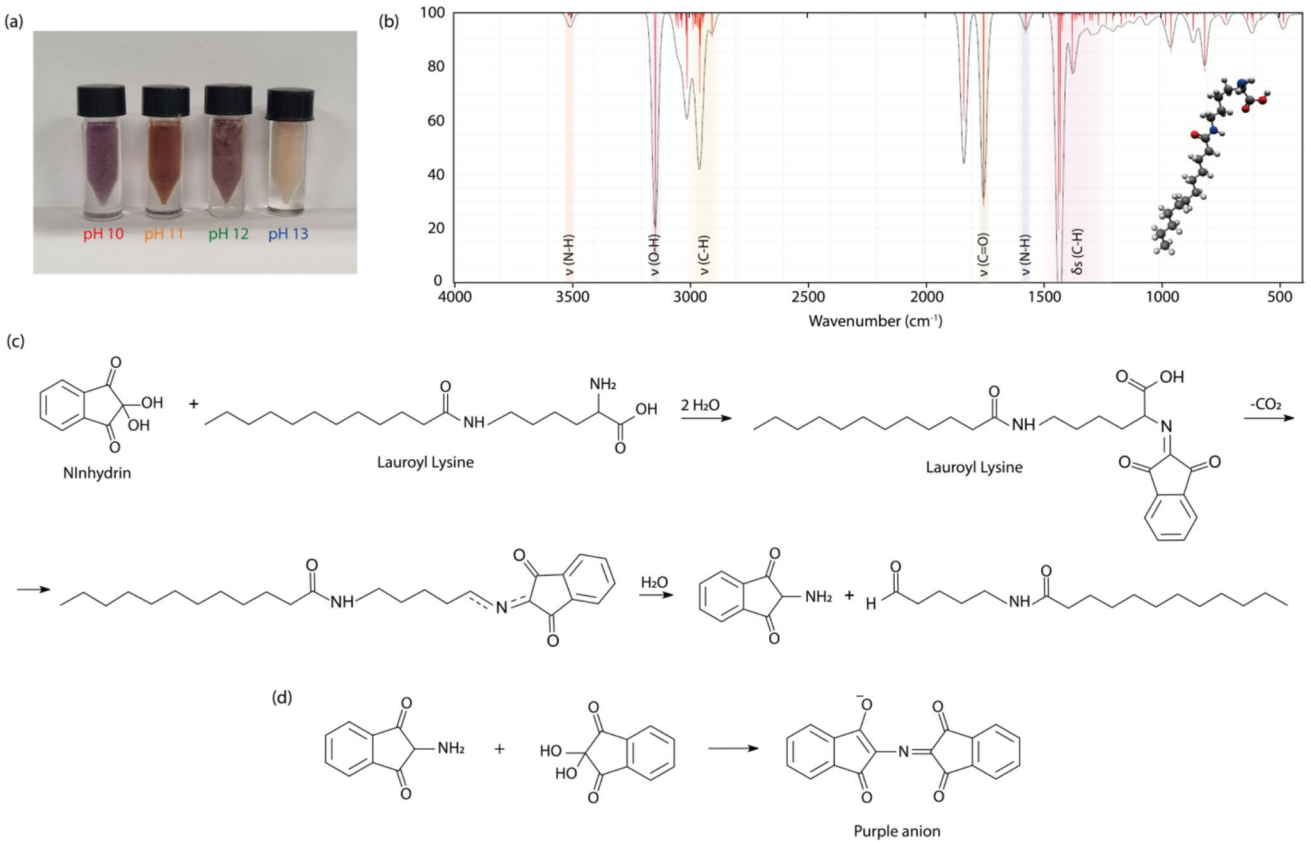

Fig. 3 Ninhydrin reaction and FTIR ab-initio simulation analysis of lauroyl lysine. **a** Ninhydrin reaction results of lauroyl lysine synthesized at different pH levels. The color changes of the samples from pH 10–13 indicate variations in amino group reactivity. **b** Ab-initio FTIR spectrum of lauroyl lysine simulated using ORCA quantum chemistry simulation suite. Characteristic peaks of key functional groups were identified and compared with experimental data. **c** Reaction mechanism between lauroyl lysine and ninhydrin, illustrating how the free amino group of lauroyl lysine interacts with ninhydrin, leading to conjugation and color observable change. **d** Formation mechanism of the purple anion conjugate product, demonstrating the reaction between ninhydrin and amines to produce the characteristic Ruhemann's purple compound

reaction between ninhydrin and amino acids, which produces a characteristic purple and amber color [28]. Since lauroyl lysine contains amino acid groups, this test evaluates the presence of such targeted amino acid derivative functional groups. The appearance of a color change upon reaction indicates the successful detection of such amino acid group [29]. By observing color changes in the test samples, the progress and outcomes of the reactions were analyzed. Activated at 80 °C, color changes gradually appear as temperature condition is suitable for causing ninhydrin test chemical reaction.

If the final amino acid derivative product retains amino acids, a ninhydrin reaction can be expected as the solution has a color change from uncolored to purple-amber brown. According to the ninhydrin test procedure, the structure of lauroyl lysine contains the amine groups of amino acids, which serve as the basis for a successful Schotten–Baumann reaction. Purple appears at pH 10, which is a typical color change that is formed when a compound containing an amino acid or amine group reacts with ninhydrin, chemically verifying that lauroyl lysine contains an amino acid [30]. At pH 11, the purple-amber color could be identified, which is a color change that can occur due to the influence of the basic amine group of amino acids as alkalinity increases, which is interpreted as an indicator of the reactivity of amino acids. At pH 12, a light purple color appeared, which indicates the presence of amino acid group of lauroyl lysine in the solution. This shows that lauroyl lysine powder does not dissolve well in water even after sufficient heating and becomes slightly less reactive. At pH 13, ivory color is observed as no color change is apparent, which is interpreted due to lysine molecular group's unfavorable attachment to the -NH_2 amine group adjacent to –COO^- in a very alkaline environment, to a state where alternate -NH_2 group adjacent to carbon chain does not actively react with ninhydrin for color conjugate to occur [31]. It suggests the possibility that at high pH, deamination of amino acids chemical changes may have occurred. The results of these experiments confirm that lauroyl lysine contains amino acid components under optimized pH condition and show that the chemical properties of amino acids or amine groups change with pH changes. In particular, the purple color at pH 10 is interpreted as an important indicator that confirms the presence of amino acid group is retained in lauroyl lysine as an amino acid derivative product.

In Fig. 3c, reaction mechanism between lauroyl lysine and ninhydrin prior to the observable color change product of Ruhemann's purple (Fig. 3d) anion is illustrated. As carbon dioxide (CO_2) is released, the number of carbon atoms in the R group is reduced, and water (H_2O) is subsequently added. Examining the molecular structure of lauroyl lysine closely, primary amide group exists at the hydrophilic end of the molecule, with the presence of both primary and secondary amine groups observed within lauroyl lysine molecular structure. The presence of the amide group structure is crucial in the ninhydrin test for lauroyl lysine. The ninhydrin test detects primary amides (α-amino acids) over secondary amides, in a sample by producing a purple or amber color. The ninhydrin reaction is specific to amino acids, because their free primary amino acid groups are required to produce the characteristic visible color absorbing organic conjugate dye Ruhemann's purple anion upon reaction with ninhydrin. In this case, since lauroyl lysine is an amino acid derivative, the presence of the amino acid group is key to the reaction.

Given that the amino acid group in lauroyl lysine is part of the amino acid lysine component, it can be affected by both the pH and the hydrophobic tail of the molecule. Following with experiment results, this would be available to explain why color changes were observed at lower pH, where the amino group is more readily available as charged zwitterion. More unconventional results were observed at pH 13, where the primary amine group may be less reactive due to unfavorable attachment toward lauroyl carbon molecule group as a secondary amide instead [32]. The unchanged ivory color at pH 13 could be explained by the strong basic condition enhancing the affinity between activated -NH_3^+ amide in the vicinity of COO^- amide groups and lauroyl chloride acyl group condensing into secondary amide molecules, reducing the reactivity with ninhydrin [33]. The fact that synthesized lauroyl lysine may undergo different reactions under varying pH solutions; this can influence the distinction between primary amides within its molecular structure.

Secondary amines with two carbon groups attached to nitrogen do not produce Ruhemann's purple color, but it can produce yellow products because of their different reaction pathways. When ninhydrin is reacted with amino acids containing secondary amines such as proline, it is reported to induce color change into a yellow solution [34]. At high pH, secondary amines are deprotonated and become more reactive under basic conditions. Consequently, it was confirmed that the functional groups in the lauroyl lysine molecule behave differently depending on the pH reaction conditions. The experimental results with lauroyl lysine are consistent with these principles. The variation in color depending on pH supports the idea that functional groups, such as primary and secondary amines, along with primary amides in the molecule respond differently under various environmental conditions. Observations of color changes at varying reaction pH conditions above the pH 9.7 isoelectric point, particularly at pH 13, suggest that amide group primary and secondary structural differences influence the ninhydrin reaction outcome.

The optimized synthesis of lauroyl lysine occurred at pH 10, where acetone filtration to successfully purify the yield product was used. Loss on drying was conducted on the optimized amino acid derivative product. In the loss on drying test, to demonstrate the stability of sample's mass

underdrying conditions, ensuring that the physical form was preserved and no significant volatile substances were lost. The drying process was conducted under heating conditions at 60 °C on dry glass petri dish. The volatile by-product mass loss was calculated as 0.70%, which meets the Japanese Pharmacopoeia (JP) protocol No. 2.41 industrial requirement where the finalized product loss should not exceed 3%. This confirms that the lauroyl lysine product maintains stability and meets industrial quality specifications. Synthesized sample was heat treated with the remaining residue after quality specification verification. JP test protocol No. 2.44 for the Residue on Ignition Test was conducted on the optimized product, where industrial requirement is not more than 1.0% residue by weight. Upon ignition, the white organic solid underwent visible thermal decomposition, accompanied by the evolution of smoke and the formation of a dark, ash-like residue. The near-complete absence of uncharred material suggests that the compound was effectively oxidized. The protocol verified the residual to be 0.06% by weight, fulfilling the industrial requirement qualifications for the optimized lauroyl lysine synthesis product.

NMR is a crucial analytical technique for determining the position of hydrogen and carbon atoms within the carbon skeleton and verifying the presence of surrounding functional groups. The ^{1}H-NMR spectrum of lauroyl lysine was recorded using a 100 MHz NMR spectrometer with deuterated dimethyl sulfoxide-d6 (DMSO-d6) as solvent (Fig. 4). The selected NMR solvent was adequate for ppm range of interest, and the solvent selection process was referred to by an analysis of NMR report. An adequate sampling amount of optimized lauroyl lysine at pH 10 was dissolved in the solvent, filtered using a PTFE syringe filter, and transferred to an NMR tube. The pretreated NMR tube was maintained in a hot block at approximately 35 °C, and 16 scans were acquired over 1 min. The chemical shifts (δ) are reported in parts per million (ppm), referenced to the residual solvent peak.

A singlet peak at 1.23 ppm is characteristic of protons in the methylene (R_2-CH_2) group [35, 36]. This peak corresponds to regions (c) ~ (i), and (p) ~ (r) in the spectrum. A peak at 0.92 ppm originates from the methyl (R-CH_3) group for (a) [37]. The spectrum exhibits aliphatic peaks from methyl and methylene (R-CH_3 and R_2-CH_2) groups, which are characteristic of hydrocarbon-containing structures. Thus, the ^{1}H-NMR signal ratio confirmed the presence of -CH_2- and -CH_3 groups at the aliphatic lauroyl carbon chain. The peak observed at 2.32 ppm is assigned to the methylene group adjacent to the amide functional group (-CH_2-CONH-), corresponding to (k). This peak appears as a triplet due to spin–spin coupling with the neighboring methylene group, which is consistent with the typical chemical shift range of 2.1–2.5 ppm for such environments. Additionally, the peak at 2.51 ppm can be attributed to (o) methylene group (-CONH-CH_2-), also

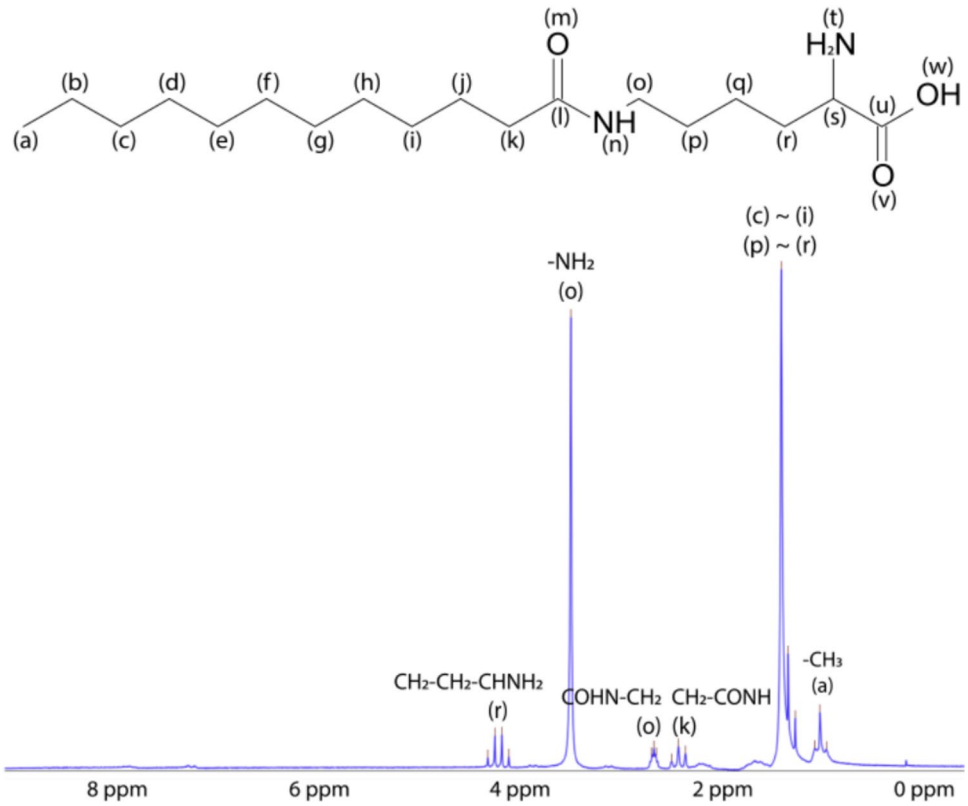

Fig. 4 ^{1}H-NMR spectrum of lauroyl lysine in DMSO-d6 solvent

appearing as a triplet. This assignment is reasonable given the expected chemical shift range for methylene groups adjacent to amide functional groups in similar compounds [38, 39].

Furthermore, the amine functional group (-NH_2) spectrum was observed matching as a (t) amine as a singlet 3.31 ppm peak. This assignment is reasonable given that the amines (-NH_2) typically appear in the range of 2.6–3.5 ppm. The observed chemical shift is consistent with previously reported values for similar amine-containing compounds, where the electronegative nitrogen induces a slight deshielding effect. The interpreted quadruplet appeared at 3.96 ppm arising from (r) methylene group (-CH_2-CH_2–$CHNH_2$) signal in vicinity of the lysine primary amide [40, 41]. DMSO is a very polar solvent that can interact with molecules with strong hydrogen-bonding ability. Particularly, since the amide (-CONH-) group contains N–H bonds, it can form hydrogen bonds and is likely to interact strongly with DMSO. Such interactions may affect the chemical shift in the NMR spectrum. Hydrogen bonding with a highly polar solvent likely shifts the -CH_2- peak of amide to the lower ppm region. That is, if the signal shown near 4.0 ppm in this study was due to the amide, it may have shifted to lower ppm due to the solvent effect [42]. Through materials' characterization, synthesized lauroyl lysine amino acid derivative organic compounds were verified through FTIR and NMR, having produced optimized final product results. NMR determined whether the carbon chain backbone structure was well formed, while FTIR was used to assess the functional group in the lauroyl lysine pH optimized product. Based on the comprehensive results of FTIR, SEM, ninhydrin test, and ^{1}H-NMR analysis, pH 10 was confirmed to be the most optimal condition for lauroyl lysine synthesis, providing the highest structural stability, crystallinity, and functional group preservation.

To evaluate process scalability under these optimized conditions, scaled-up synthesis was performed by increasing the reactant concentration by a factor of 2 (40 mmol), 3 (60 mmol), and 4 (80 mmol) while maintaining the same reaction time (1 h) and pH. The injection rate of lauroyl chloride was proportionally adjusted to 0.16, 0.23, and 0.31 mL/min, respectively, to ensure complete addition within a fixed time. As a result, yields of 9.68 g (94.06%) at 2 × scale, 14.32 g (92.76%) at 3 × scale, and 18.71 g (90.84%) at 4 × scale were obtained. These results demonstrate that the lauroyl lysine synthesis protocol is scalable under continuous flow conditions and maintains high yield and purity as the reaction volume increases. However, a slight decrease in efficiency was observed at large scales due to increased reaction complexity.

Conclusions

Lauroyl lysine was synthesized in this study by reacting lauroyl chloride to L-lysine, and the synthesis efficiency and product yield were compared under pH conditions ranging from 10 to 13. The reaction proceeded based on the Schotten–Baumann mechanism, with lauroyl chloride continuously injected at a rate of 0.08 mL/min for 1 h. According to the yield analysis, the highest yield (97.77%) was obtained at pH 10, with a gradual decrease observed as pH increased. The yields at pH 11, 12, and 13 were 80.16%, 72.51%, and 55.20%, respectively. In Fig. 1c, the amount of solid precipitate also decreased as the pH increased. FTIR analysis confirmed characteristic peaks indicating the formation of amide bonds, and ^{1}H-NMR spectra revealed specific proton environments corresponding to the lauroyl lysine structure. SEM analysis showed that the synthesized product at pH 10 exhibited relatively uniform particle morphology, while higher pH conditions led to increased surface aggregation and amorphous structures. Furthermore, the presence of amino groups in the lauroyl lysine products was confirmed through the ninhydrin reaction, with the most distinct color change observed at pH 10. Based on these results, pH 10 was determined to be the most suitable condition for the synthesis of lauroyl lysine. Increasing the pH led to a decrease in yield and structural changes in the product. This study provides fundamental experimental data for optimizing reaction conditions in the synthesis of lauroyl lysine under continuous flow reaction as alternative to batch-type reactions. To further evaluate the scalability of the optimized condition (pH 10), scale-up syntheses were carried out at twofold (40 mmol), threefold (60 mmol), and fourfold (80 mmol) scales. The isolated product yields were 9.68 g (94.06%), 14.32 g (92.76%), and 18.71 g (90.84%), respectively. These results indicate that the reaction is reproducible and maintains high efficiency at larger scales, although a slight decrease in yield was observed as the reaction scale increased.

Funding The work of Shin Hum Cho was supported by Bisa Research Grant of Keimyung University, under Grant No. 20220648.

Data availability The data is available upon request to the authors.

Declarations

Conflict of interest The authors declare no competing financial interests.

References

1. S. Jeong, Y. Jeon, J. Mun, S.M. Jeong, H. Liang, K. Chung, P.-I. Yi, B.-S. An, S. Seo, Ninhydrin loaded microcapsules for detection of natural free amino acid. Chemosensors **11**(1), 49 (2023). https://doi.org/10.3390/chemosensors11010049
2. J.P. Perdew, K. Burke, M. Ernzerhof, Generalized gradient approximation made simple. Phys. Rev. Lett. **77**(18), 3865–3868 (1996). https://doi.org/10.1103/PhysRevLett.77.3865
3. D.B. Tripathy, A. Mishra, J. Clark, T. Farmer, Synthesis, chemistry, physicochemical properties and industrial applications of amino acid surfactants: a review. C. R. Chim. **21**(2), 112–130 (2018). https://doi.org/10.1016/j.crci.2017.11.005
4. N.A. Bowden, J.P.M. Sanders, M.E. Bruins, Solubility of the proteinogenic α-amino acids in water, ethanol, and ethanol-water mixtures. J. Chem. Eng. Data **63**(3), 488–497 (2018). https://doi.org/10.1021/acs.jced.7b00486
5. G. Haeger, J. Wirges, J. Bongaerts, U. Schörken, P. Siegert, Perspectives of aminoacylases in biocatalytic synthesis of N-acyl-amino acids surfactants. Appl. Microbiol. Biotechnol. **108**(1), 1–19 (2024). https://doi.org/10.1007/s00253-024-13328-7
6. M.C. Bourkaib, S. Delaunay, X. Framboisier, L. Hôtel, B. Aigle, C. Humeau, Y. Guiavarc'h, I. Chevalot, N-acylation of L-amino acids in aqueous media: evaluation of the catalytic performances of *Streptomyces Ambofaciens* Aminoacylases. Enzyme Microb. Technol. **137**, 109536 (2020). https://doi.org/10.1016/j.enzmictec.2020.109536
7. E.N. Vulfson, *Enzymes in nonaqueous solvents: methods and protocols* (Springer Science & Business Media, Cham, 2008)
8. L.P. Kozlowski, IPC 2.0: Prediction of isoelectric point and pKa dissociation constants. Nucleic Acids Res. **49**(W1), W285–W292 (2021). https://doi.org/10.1093/nar/gkab295
9. B. Zwanenburg, M. Mikołajczyk, P. Kiełbasiński, *Enzymes in action green solutions for chemical problems: green solutions for chemical problems* (Springer Science & Business Media, Cham, 2000)
10. M. Koreishi, R. Kawasaki, H. Imanaka, K. Imamura, Y. Takakura, K. Nakanishi, Efficient *N*ε-lauroyl-l-lysine production by recombinant ε-lysine acylase from *Streptomyces Mobaraensis*. J. Biotechnol. **141**(3), 160–165 (2009). https://doi.org/10.1016/j.jbiotec.2009.03.008
11. A. Pinazo, L. Pérez, M. Lozano, M. Angelet, M.R. Infante, M.P. Vinardell, R. Pons, Aggregation properties of diacyl lysine surfactant compounds: hydrophobic chain length and counterion effect. J. Phys. Chem. B **112**(29), 8578–8585 (2008). https://doi.org/10.1021/jp802193p
12. S. Kaplan, M. Colak, H. Hosgoren, N. Pirinccioglu, Design of L-lysine-based organogelators and their applications in drug release processes. ACS Omega **4**(7), 12342–12356 (2019). https://doi.org/10.1021/acsomega.9b01086
13. A.P. Mikhalkin, The synthesis, properties, and applications of N-acyl-α-aminoacids. Russ. Chem. Rev. **64**(3), 259 (1995). https://doi.org/10.1070/RC1995v064n03ABEH000149
14. E.C. Izgu, A. Björkbom, N.P. Kamat, V.S. Lelyveld, W. Zhang, T.Z. Jia, J.W. Szostak, N-carboxyanhydride-mediated fatty acylation of amino acids and peptides for functionalization of protocell membranes. J. Am. Chem. Soc. **138**(51), 16669–16676 (2016). https://doi.org/10.1021/jacs.6b08801
15. P. Patil, A. Pratap, Choline chloride catalyzed amidation of fatty acid ester to monoethanolamide: a green approach. J. Oleo Sci. **65**(1), 75–79 (2016). https://doi.org/10.5650/jos.ess15070
16. M. Aydın, Z. Kartal, Ş Osmanoğlu, M. Halim Başkan, R. Topkaya, EPR and FT-IR spectroscopic studies of l-lysine monohydrochloride and l-glutamic acid hydrochloride powders. J. Mol. Struct. **994**(1), 150–154 (2011). https://doi.org/10.1016/j.molstruc.2011.03.010
17. Q. Li, J. Zhang, G. Zhang, B. Xu, L-lysine-based gelators for the formation of oleogels in four vegetable oils. Molecules **27**(4), 1369 (2022). https://doi.org/10.3390/molecules27041369
18. F. Novelli, A. Strofaldi, S. De Santis, A. Del Giudice, S. Casciardi, L. Galantini, S. Morosetti, N.V. Pavel, G. Masci, A. Scipioni, Polymorphic self-organization of lauroyl peptide in response to pH and concentration. Langmuir **36**(14), 3941–3951 (2020). https://doi.org/10.1021/acs.langmuir.9b02924
19. F. Han, Z. Song, T. Cao, M. Guo, Synthesis and properties of pH-dependent gemini surfactant containing tripeptide structure. J. Surfactants Deterg. **28**(1), 189–199 (2025). https://doi.org/10.1002/jsde.12790
20. H. Gaweska, M.H. Pozzi, D.M.Z. Schmidt, D.G. McCafferty, P.F. Fitzpatrick, Use of pH and kinetic isotope effects to establish chemistry as rate-limiting in oxidation of a peptide substrate by LSD1. Biochemistry **48**(23), 5440–5445 (2009). https://doi.org/10.1021/bi900499w
21. M.C. Bourkaib, S. Delaunay, X. Framboisier, C. Humeau, J. Guilbot, C. Bize, E. Illous, I. Chevalot, Y. Guiavarc'h, Enzymatic synthesis of N-10-undecenoyl-phenylalanine catalysed by aminoacylases from *Streptomyces Ambofaciens*. Process Biochem. **99**, 307–315 (2020). https://doi.org/10.1016/j.procbio.2020.09.009
22. Polymorphic self-organization of lauroyl peptide in response to pH and concentration. ResearchGate. https://www.researchgate.net/publication/339639306_Polymorphic_Self-Organization_of_Lauroyl_Peptide_in_Response_to_pH_and_Concentration. Accessed 31 Mar 2025
23. T.-T. Shi, Z. Fang, W.-B. Zeng, Z. Yang, W. He, K. Guo, Design, synthesis and properties investigation of N^{α}-acylation lysine based derivatives. RSC Adv. **9**(13), 7587–7593 (2019). https://doi.org/10.1039/C9RA00213H
24. H. Bouzid, A new approach on the amino acid lysine quantification by UV-visible spectrophotometry. Rev. Chim. **71**(8), 159–175 (2020)
25. R. Kembaren, J.M. Kleijn, J.W. Borst, M. Kamperman, A.H. Hofman, Enhanced stability of complex coacervate core micelles following different core-crosslinking strategies. Soft Matter **18**(15), 3052–3062 (2022). https://doi.org/10.1039/D2SM00088A
26. A.Y. El-Moghazy, N. Amaly, G. Istamboulie, N. Nitin, G. Sun, A signal-on electrochemical aptasensor based on silanized cellulose nanofibers for rapid point-of-use detection of ochratoxin A. Microchim. Acta **187**(9), 535 (2020). https://doi.org/10.1007/s00604-020-04509-y
27. T. Román, G. Acosta, C. Cárdenas, B.G. de la Torre, F. Guzmán, F. Albericio, Protocol for facile synthesis of Fmoc-N-Me-AA-OH using 2-CTC resin as temporary and reusable protecting group. Methods Protoc. **6**(6), 110 (2023). https://doi.org/10.3390/mps6060110
28. S. Medaglia, Á. Morellá-Aucejo, M. Ruiz-Rico, F. Sancenón, L.A. Villaescusa, R. Martínez-Máñez, M.D. Marcos, A. Bernardos, Antimicrobial surfaces: stainless steel functionalized with the essential oil component vanillin. Int. J. Mol. Sci. **25**(22), 12146 (2024). https://doi.org/10.3390/ijms252212146
29. E. Lange, F. Carlysle-Davies, Presumptive drug identification by ninhydrin fingerprint analysis. Forens. Chem. **40**, 100597 (2024). https://doi.org/10.1016/j.forc.2024.100597
30. A. Croitoriu, A.P. Chiriac, A.G. Rusu, A. Ghilan, D.E. Ciolacu, I. Stoica, L.E. Nita, Morphological evaluation of supramolecular soft materials obtained through co-assembly processes. Gels **9**(11), 886 (2023). https://doi.org/10.3390/gels9110886
31. T. Zhang, A. Dravid, J. Reddy, L. Aliyu, J. Park, Z. Wang, K.-W. Huang, J. Wu, S. Liu, A. Stone, M. Betenbaugh, M. Donohue, Modeling solubilities for amino acids in water as functions of

temperature and pH. Ind. Eng. Chem. Res. **63**(50), 22076–22086 (2024). https://doi.org/10.1021/acs.iecr.3c00365
32. N. Kitadai, T. Yokoyama, S. Nakashima, ATR-IR spectroscopic study of L-lysine adsorption on amorphous silica. J. Colloid Interface Sci. **329**(1), 31–37 (2009). https://doi.org/10.1016/j.jcis.2008.09.072
33. S. Hidayat, R. Benchawattananon, L. Taemaitree, Visual detection of cyanide using ninhydrin coated paper. Heliyon **11**(3), e42283 (2025). https://doi.org/10.1016/j.heliyon.2025.e42283
34. U. Boas, S. Mirsharghi, Color test for selective detection of secondary amines on resin and in solution. Org. Lett. **16**(22), 5918–5921 (2014). https://doi.org/10.1021/ol502936d
35. D. Courtier-Murias, A.J. Simpson, C. Marzadori, G. Baldoni, C. Ciavatta, J.M. Fernández, E.G. López-de-Sá, C. Plaza, Unraveling the long-term stabilization mechanisms of organic materials in soils by physical fractionation and NMR spectroscopy. Agr Ecosyst Environ **171**, 9–18 (2013). https://doi.org/10.1016/j.agee.2013.03.010
36. D. Puhan, M.T.L. Casford, P.B. Davies, Evaluation of structural and compositional changes of a model monoaromatic hydrocarbon in a benchtop hydrocracker using GC, FTIR, and NMR spectroscopy. ACS Omega **8**(39), 35988–36000 (2023). https://doi.org/10.1021/acsomega.3c03833
37. J.P. Hindmarsh, J. Prasad, P. Gopal, H. Singh, NMR measurement of bacteria death kinetics during heat stress. LWT Food Sci. Technol. **60**, 876–880 (2015). https://doi.org/10.1016/j.lwt.2014.09.060
38. G. Fischetti, N. Schmid, S. Bruderer, B. Heitmann, A. Henrici, A. Scarso, G. Caldarelli, D. Wilhelm, A deep learning framework for multiplet splitting classification in 1H NMR. J. Magn. Reson. **373**, 107851 (2025). https://doi.org/10.1016/j.jmr.2025.107851
39. J.C. Hamill Jr., J.C. Sorli, I. Pelczer, J. Schwartz, Y.-L. Loo, Acid-catalyzed reactions activate DMSO as a reagent in perovskite precursor inks. Chem. Mater. **31**(6), 2114–2120 (2019). https://doi.org/10.1021/acs.chemmater.9b00019
40. R. Triki, A. Bougarech, M. Tessier, S. Abid, A. Fradet, M. Abid, Furanic-aliphatic polyesteramides by bulk polycondensation between furan-based diamine, aliphatic diester and diol. J. Polym. Environ. **26**(3), 1272–1278 (2018). https://doi.org/10.1007/s10924-017-1037-y
41. E. Métay, M.C. Duclos, S. Pellet-Rostaing, M. Lemaire, R. Kannappan, C. Bucher, E. Saint-Aman, C. Chaix, Synthesis and conformational analysis of redox-active ferrocenyl-calixarenes. Tetrahedron **65**(3), 672–676 (2009). https://doi.org/10.1016/j.tet.2008.11.032
42. T. Zhao, Y. Zhang, G. Peng, Y. Chen, A branched hydrophobicity associated with polyacrylamide based on silica: synthesis and solution properties. J. Polym. Res. **26**(11), 250 (2019). https://doi.org/10.1007/s10965-019-1883-5